

An Optimized Energy-Harvesting Transmission Scheme for Diffusion-Based Molecular Communications

V. Musa, *Student Member, IEEE*, G. Piro, *Member, IEEE*,
L. A. Grieco, *Senior Member, IEEE*, and G. Boggia, *Senior Member, IEEE*

Abstract—In this paper, we propose an optimized transmission scheme with energy-harvesting for a diffusion-based molecular communication system composed by nano-devices fed by piezoelectric nanogenerators. To this end, we firstly derive a system model that analytically describes the mean and the variance of the aggregated noise at the output of the receiver and the achievable Bit Error Rate. Then, we formulate an optimization problem that minimizes an objective function defined as a linear combination of the probability that the voltage across the ultra-nanocapacitor of the transmitter goes under a target value and the number of enqueued packets. We solve this problem by considering the actual energy budget, a target Bit Error Rate, and the need to achieve the simplicity of the transmitter as constraints. Finally, we use computer simulations to validate the formulated analytical models and demonstrate the unique ability of the proposed approach to guarantee $BER = 5\%$ and $BER = 10\%$ for communication distances up to $47\mu m$ and $50\mu m$, respectively, while registering better results against baseline scenarios.

Index Terms—Diffusion-based molecular communications, energy-harvesting, system model, optimization.

I. INTRODUCTION

Diffusion-based molecular communications are emerging as a groundbreaking solution to deploy interconnected systems at the nanoscale, enabling pioneering services in medical, industrial, and environmental application domains [1]. By encoding and delivering the binary information through different modulation schemes (concentration-based [2], molecule type-based [3], release time-based [4], and spatial domain-based [5]), transmitter nano-devices consume a non-negligible amount of energy (e.g., 100 zJ for 5000 transmitted molecules) [6], [7]. Accordingly, optimized mechanisms with energy-harvesting become fundamental to achieve long lasting and effective communications among nano-devices fed by nano-batteries with limited capacity [2].

Different scientific contributions formulated optimization problems for improving the performance of diffusion-based molecular communication systems [6], [8]–[16]. Some of these works assumed to limit the number of molecules [10]–[14] or the amount of energy consumed by the transmitter nano-device [6] for each symbol. But, none of them considered the integration of energy-harvesting mechanisms. To the best

of authors' knowledge, only [17] and [18] investigated the adoption of Zinc Oxide (ZnO)-based piezoelectric nanogenerators in diffusion-based molecular communication systems. The resulting transmission solution, however, did not consider any optimized transmission technique and failed to preserve the simplicity of the transmitter.

To provide an important step forward in this promising research topic, we present in this paper a novel methodology that optimizes a diffusion-based molecular communication system composed of nano-devices fed by ZnO-based piezoelectric nanogenerators. Without loss of generality, this study focuses on a telemedicine use case, where implanted nano-devices collect healthcare information directly from the human body and occasionally transmit them to a remote monitoring device.

The main scientific contributions of this work are summarized in what follows. First, starting from existing studies describing (i) diffusion noise and inter-symbol interference at the input of the receiver [19] and (ii) the linearized ligand-receptor model [20], this work provides an analytical formulation of the mean and the variance of the aggregated noise at the output of the receiver in order to compute the error probability. Second, by modeling the transmission process with a current generator, as in [18], we derive the probability that the voltage across the ultra-nanocapacitor goes under a target value and the number of enqueued packets, based on the transmission process behavior, to properly formulate the optimization problem. Third, we conceive a novel optimization problem to dynamically select the load current among a very limited subset of possible values on a per-frame basis, while satisfying energy constraints and target Bit Error Rate (BER). According to [12], the optimization problem is solved by a remote nano-device interacting with the transmitter nano-device through an out-of-band communication technique that, despite out-of-scope of this work, further ensures the transmitter simplicity. Fourth, computer simulations are used to validate the proposed analytical models and demonstrate that the conceived methodology always satisfies the expected performance levels in conceivable scenarios with different configuration parameters.

The rest of this work is organized as follows. Section II discusses the state-of-the-art on solutions targeting long-lasting communication capabilities or formulating optimization problems for diffusion-based molecular communications. Section III describes the considered system model, analyzing the aggregated noise at the output of the receiver and the

The authors are with the Department of Electrical and Information Engineering (DEI), Politecnico di Bari, 70126 Bari, Italy, and also with the Consorzio Nazionale Interuniversitario per le Telecomunicazioni (CNIT), 43124 Parma, Italy. E-mail: {vittoria.musa, giuseppe.piro, alfredo.grieco, gennaro.boggia}@poliba.it.

resulting BER. Section IV presents the conceived optimization problem. Section V illustrates the numerical results. Finally, Section VI draws the conclusions of the work and summarizes future research activities.

II. STATE OF THE ART

In diffusion-based molecular communications, the generation, release, and reception of information molecules cause a non-negligible amount of energy consumption [6], [7]. This section reviews the scientific works addressing this important aspect, while also highlighting the *literature gaps* that our contribution intends to overcome.

Initial solutions targeting long-lasting communication capabilities at both micro and nanoscales envisage to refill the transmitter reservoir by retrieving information molecules from the surrounding environment [21]–[24]. These works, however, do not consider all the energy needs related to the communication process and the actual energy budget available within nano-devices (*first literature gap*).

Differently, energy-harvesting techniques can be used to retrieve energy from mechanical [25], [26] and chemical [27], [28] sources available in the surrounding environments. Piezoelectric nanogenerators, composed of ZnO [25] or lead zirconate titanate (PZT) [26] nanowires, for instance, retrieve electrical energy from external vibrations. Unfortunately, most of contributions in this context do not consider diffusion-based molecular communications (*second literature gap*): they investigated the adoption of piezoelectric nanogenerators to feed nano-devices communicating through electromagnetic waves in wireless nano-sensors networks at the Terahertz band [29]–[31] or to selectively stimulate peripheral nerves in the human body through light signals [32], [33].

Regarding diffusion-based molecular communications, piezoelectric nanogenerators have been proposed to feed nano-devices only in [17], [18]. These works proposed a power control mechanism based on a closed-loop control scheme, where the amount of molecules to transmit is set proportional to the available energy budget. By modeling the transmission process through a current generator, they assumed to select any load current value within a range that ensures global asymptotic stability and target performance. Instead, to preserve the transmitter simplicity, it would be desirable to select the load current among few available possibilities, e.g., through an optimized approach (*third literature gap*).

The optimization theory has been used in diffusion-based molecular communications to improve transmission efficiency [6], [8], increase the quality of the received signal [9], find the optimal threshold or detection scheme minimizing the error probability [10], and optimize the resource allocation in multi-user scenarios [11]–[13], as well as to find the optimum relay position [15] and the optimal number of transmitted molecules [14], [16] that minimize the BER in cooperative and mobile networks. Here, only [6], [10]–[14] propose to optimize transmission settings by considering an initial available energy budget. However, none of them investigate the adoption of energy-harvesting mechanisms, which produce a variation of the available energy budget over time, and look at the transmitter simplicity (*fourth literature gap*).

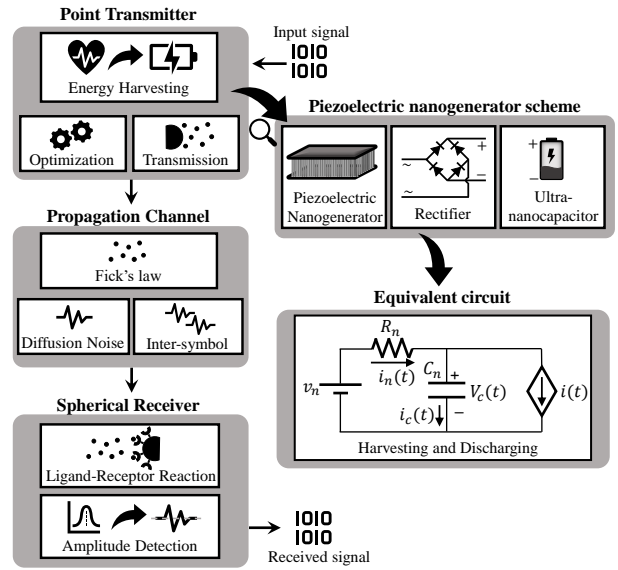


Fig. 1. The considered molecular communication system model, including a point transmitter fed by piezoelectric nanogenerator and a spherical receiver.

To bridge all these gaps, we propose a novel, optimal, and energy-harvesting transmission scheme for a diffusion-based molecular communication system, allowing to preserve the simplicity of the transmitter by selecting the amount of energy to be consumed for communication purposes among few possible values, while also considering both performance and energy constraints.

III. THE SYSTEM MODEL

This work focuses on a pioneering telemedicine use case, enabled by diffusion-based molecular communications, where implanted nano-devices deliver biological information on demand (i.e., when there is a significant variation in the measured value or when the doctor visits the patient). The considered system includes a point transmitter fed by a piezoelectric nanogenerator, an aqueous propagation medium where molecules freely diffuse, and a spherical receiver equipped with homogeneously distributed receptors (see Fig. 1). Depending on the specific scenario, nano-device may 1) follow the bloody stream and communicate with a fixed receiver every cycle, 2) send information only when there is a significant variation in the measured value, or 3) transmit information when the doctor visits the patient. Indeed, to model the bursty nature of the communication process, we also assume that the transmitter sends information molecules only during constant ON times, while staying silent for OFF time periods t_{OFF} (see Fig. 2). The transmitter uses the On-Off Keying (OOK) modulation (i.e., the most suitable transmission scheme for constrained and nanoscale devices [2]) to release Q or zero molecules for 1-bits and 0-bits, respectively. The symbol duration is denoted with T_s , while the time interval T_b required to release a burst of molecules is much smaller than T_s , that is $T_b \ll T_s$. Let T_f be the frame duration. The t_{ON} period allows transmitting M consecutive frames of N bits: $t_{ON} = MT_f$, $T_f = NT_s$. The duration of OFF periods can be described through an exponential random variable.

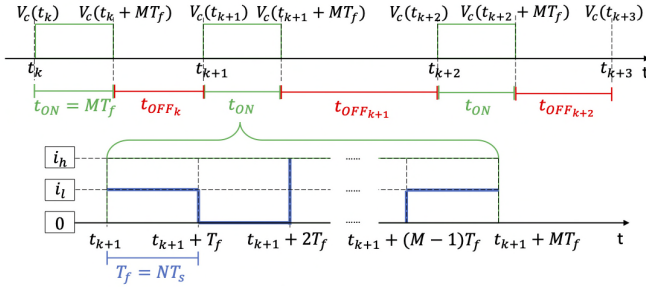


Fig. 2. The transmission model with ON periods, composed by M frames, and variable OFF periods.

In what follows, Section III-A summarizes the main theoretical results that are at the basis of the developed approach. Then, Section III-B further enriches the reference system model by analytically deriving the mean and variance of the aggregated noise at the output of the receiver and the resulting BER, essential for formulation of the performance constraint to be considered by the optimization problem in Section IV. Note that most of the considered variables depend on the communication distance, d . This dependence, however, is omitted to simplify the notation.

A. Models for Transmitter, Propagation, and Reception

We suppose that transmitter and receiver are synchronized according to [34]. The transmitter hosts a piezoelectric nanogenerator composed of arrays of ZnO nanowires which, excited by vibrations due to the human heartbeat, provides energy to system communication procedures [25], [29], [30], [32], [33]. In line with [18], the harvesting and discharging processes are modeled through the equivalent circuit depicted in Fig. 1. The harvesting process is represented by an ideal voltage source, v_n , in series with a resistor, R_n , and an ultra-nanocapacitor with capacitance C_n and voltage $V_c(t)$ [29]. The voltage source generates an electric charge h_n every cycle time t_n , where h_n considers the loss due to the conversion between mechanical and electrical energy [29]. On the other hand, the discharging process is modeled with a current source (i.e., the load current $i(t)$) in parallel with the ultra-nanocapacitor [17], [18]. The discrete-time state equation of the harvesting and discharging system is [18]:

$$V_c(t_{j+1}) = V_c(t_j) e^{-\frac{T_f}{R_n C_n}} + \left(e^{-\frac{T_f}{R_n C_n}} - 1 \right) \left(i(t_j) R_n - v_n \right), \quad (1)$$

where T_f corresponds to the frame duration and t_j is the initial time instant of the j -th frame, that is $t_j = t_k + (j-1)T_f$ with $j \in [1, M]$. The transmission power spent during the j -th frame, $p(t_j)$, is computed by considering the conversion rate ξ of the electrochemical process used to recover chemical energy from the electrical energy stored in the ultra-nanocapacitor [35], [36], the voltage across the ultra-nanocapacitor at the beginning of the j -th frame, $V_c(t_j)$, and the chosen load current, $i(t_j)$, that is:

$$p(t_j) = \xi V_c(t_j) i(t_j). \quad (2)$$

The resulting consumed energy, that is $E_c(t_j) = p(t_j)T_f$, is used to generate the information molecules related to the j -th

frame. The amount of energy required to generate and release a burst of molecules is assumed to be comparable with respect to the one consumed by pure biological systems using diffusion-based molecular communications [6].

The emitted molecules freely diffuse in a fluid medium. Since the concentration of emitted particles is typically much lower than the medium particle concentration, the molecules displacement is modeled by a Brownian motion, according to which information particles diffuse independently from each other and their motion is affected by the diffusion coefficient D . Considering a burst of Q released molecules, the molecule concentration at distance d and time t is derived by the Fick's law of diffusion [37]: $c(t) = Q(4\pi Dt)^{-3/2} e^{-d^2/(4Dt)}$.

The concentration of molecules reaching the receiver is affected by the diffusion noise and inter-symbol interference [19]. The diffusion noise, $n_D(t)$, is due to collisions of information molecules with each other and with the fluid particles in the propagation medium. It can be modeled as a Poisson and additive noise [19]. However, considering a large number of emitted molecules, it can be approximated by a Gaussian distribution [38]. Accordingly, the diffusion noise is described by an additive Gaussian noise with zero mean and variance depending on the measured signal: $n_D(t) \sim \mathcal{N}(0, \sigma_D^2(t))$. According to [19], the variance of the diffusion noise is computed as $\sigma_D^2(t) = c(t)/V_{rx}$, where $c(t)$ is derived by the Fick's law of diffusion and V_{rx} is the receiver volume. The inter-symbol interference, $n_I(t)$, instead, is generated by the molecular concentration related to the previously transmitted symbols. It is modeled as a Gaussian random variable, i.e., $n_I(t) \sim \mathcal{N}(\alpha, \beta)$, where the mean α and the variance β depend on the communication distance, the number of emitted molecules, the propagation medium properties, and the adopted transmitter and receiver [39]. In what follows, the mean and variance of the inter-symbol interference are numerically derived. Indeed, the actual concentration of molecules reaching the receiver side at distance d and time t is equal to $c_r(t) = c(t) + n_D(t) + n_I(t)$.

The molecule concentration reaching the receiver sphere interact with the receptor placed on the receiver surface, according to the ligand-receptor reaction [40]. Without loss of generality, this work considers a widely accepted receiver model based on the ligand-receptor reaction proposed in [2], that represents a recent highly-cited work. However, with few adjustments, the results of this work may be extended to other reactive receiver models as well. According to [2], hence, the variation of the number of molecules really captured by the receiver, $z_r(t)$, is given by the following non-linear receiver model $dz_r(t)/dt = k_f R c_r(t) - k_f c_r(t) z_r(t) - k_r z_r(t)$, where R is the number of receptors, k_f is the forward reaction rate, k_r is the reverse reaction rate. However, assuming $k_f \ll k_r$, the non-linear term $k_f c_r(t) z_r(t)$ can be neglected and the receiver model becomes linear, that is $dz_r(t)/dt = k_f R c_r(t) - k_r z_r(t)$. Considering its Fourier transform, the receiver is modeled as a low-pass filter with transfer function $H(f)$ and pulse response $h(t)$:

$$H(f) = \frac{k_f R}{k_r + j2\pi f}; \quad h(t) = k_f R e^{-k_r t} u(t). \quad (3)$$

Finally, the received signal is sampled to detect the maximum number of molecules received in each time slot and it is compared with a given threshold, Θ . If the measured signal is higher than Θ , the receiver assumes that the received bit is equal to 1, otherwise the symbol is decoded as 0. Then, the optimal sampling time is derived by considering the closed-form solution of the linear ligand-receptor reaction when the received concentration of molecules is only related to the emitted signal (i.e., $c_r(t) = c(t)$) without noise contributions, that is $dz_r(t)/dt = k_f Rc(t) - k_r z_r(t)$ with initial conditions $c(t=0) = 0$ and $z_r(t=0) = 0$. Accordingly, $z_r(t) = e^{-k_r t} k_f R \int_0^t c(\tau) e^{k_r \tau} d\tau$, where $c(t)$ is the result of the Fick's law of diffusion. The optimal sampling time T , corresponding to the maximum received signal without noise C_{max} , is obtained by numerically evaluating the time instant in which the first time derivative of $z_r(t)$, that is $dz_r(t)/dt = k_f Rc(t) - k_r z_r(t)$, is equal to 0.

B. Developed Noise Model

The performance of the considered system is evaluated in terms of error probability. To properly evaluate the average BER, it is necessary to quantify the mean and the variance of the aggregated noise at the output of the receiver. The noise at the input of the receiver, n_{in} , is composed by the sum of two independent Gaussian random variables (i.e., the diffusion noise, n_D , and the inter-symbol interference, n_I). Hence, the aggregated noise at the output of the receiver, n_{out} , is obtained by filtering n_{in} with the low-pass filter described in (3).

Theorem 1: Let α , k_f , k_r , and R be the mean of the inter-symbol noise at the input of the receiver, the forward reaction rate, the reverse reaction rate, and the number of receptors around the receiver sphere, respectively. Then, the mean of the noise at the output of the receiver is:

$$\mu_{out} = \alpha \frac{k_f R}{k_r}. \quad (4)$$

Proof: The sum of two independent Gaussian random variable (i.e., n_D and n_I) is still a Gaussian random variable with mean equal to the sum of the two means and variance equal to the sum of the two variances, that is $n_{in}(t) \sim \mathcal{N}(\alpha, \beta + \sigma_D^2(t))$ [20]. Thus, given the pulse response $h(t)$ derived in (3), the mean at the output of the receiver can be evaluated as $\mu_{out} = \alpha * h(t) = \alpha H(0) = \alpha k_f R / k_r$. ■

Theorem 2: Let k_f , k_r , R , β , D , Q , V_{rx} , d , T , and b be the forward reaction rate, the reverse reaction rate, the number of receptors, the variance of the inter-symbol interference at the input of the receiver, the diffusion coefficient of the propagation medium, the number of emitted molecules for 1-bits, the volume of the receiver, the communication distance, the sampling time, and the transmitted bit, respectively. Then, the variance of the noise at the output of the receiver is:

$$\sigma_{out}^2 = \begin{cases} \frac{\beta k_f^2 R^2}{k_r^2}, & \text{if } b = 0 \\ \frac{k_f^2 R^2}{k_r} \left[\frac{\beta}{k_r} + \frac{Q}{V_{rx} (4\pi D)^{\frac{3}{2}}} e^{-k_r T} \Gamma(T) \right], & \text{if } b = 1 \end{cases} \quad (5)$$

where $\Gamma(T) = \int_0^T (e^{-d^2/(4D\nu)} / \nu^{\frac{3}{2}}) e^{k_r \nu} d\nu$.

Proof: Let $w(t)$ be a normal random variable (i.e., $w(t) \sim \mathcal{N}(0, 1)$). Considering the relationship between a Gaussian random variable and a normal random variable, the noise at the input of the receiver can be written as $n_{in}(t) = \alpha + \sqrt{\beta + \sigma_D^2(t)} w(t)$. The autocorrelation of the noise at the input of the receiver is computed by considering two time instant, t_1 and t_2 , with $t_2 \geq t_1$:

$$\begin{aligned} R_{n_{in}}(t_1, t_2) &= E[n_{in}(t_1) \cdot n_{in}(t_2)] \\ &= \alpha^2 + \left(\beta + \sqrt{\sigma_D^2(t_1) \sigma_D^2(t_2)} \right) \delta(t_2 - t_1). \end{aligned} \quad (6)$$

Since the autocorrelation in (6) depends on the considered time instant, t_1 and t_2 , the noise process is not wide-sense stationary. Therefore, the autocorrelation at the output of the receiver is computed as $h(t_1) * h(t_2) * R_{n_{in}}(t_1, t_2)$, where $h(t_1)$ and $h(t_2)$ are the pulse response of the receiver, evaluated in t_1 and t_2 , respectively. Considering that the term multiplied by the delta function in (6) is different from zero only if $t_1 = t_2$, the autocorrelation of the noise at the output of the receiver, that is $R_{n_{out}}(t_1, t_2)$, is derived in (7).

Now, the power of the noise at the output of the receiver, $P_{n_{out}}$, can be computed by evaluating the autocorrelation at the output when $t_1 = t_2 = T$ (where T is the sampling time instant), that is: $P_{n_{out}} = R_{n_{out}}(T, T)$. Hence, by evaluating the (7) for $t_1 = t_2 = T$ and remembering that $\sigma_D^2(t) = c(t)/V_{rx} = Q(4\pi Dt)^{-3/2} e^{-d^2/(4Dt)} / V_{rx} u(t)$ (see Section III-A), $P_{n_{out}}$ can be written as:

$$P_{n_{out}} = \frac{k_f^2 R^2}{k_r} \left[\frac{\alpha^2}{k_r} + \frac{\beta}{k_r} + \frac{Q}{(4\pi D)^{3/2} V_{rx}} e^{-k_r T} \Gamma(T) \right], \quad (8)$$

where $\Gamma(T) = \int_0^T (e^{-d^2/(4D\nu)} / \nu^{\frac{3}{2}}) e^{k_r \nu} d\nu$. Then, the variance of the noise at the output of the receiver is equal to:

$$\sigma_{out}^2 = P_{n_{out}} - \mu_{out}^2, \quad (9)$$

where the autocorrelation of the noise at the output of the receiver and the resulting variance strongly depend on the transmitted bit b . Finally, the proof can be easily concluded by substituting (4) and (8) in (9). ■

To sum up, the aggregated noise at the output of the receiver is obtained by filtering the noise at the input with the ligand-receptor process and it is modeled as a Gaussian random variable with mean μ_{out} and variance σ_{out}^2 , that is $n_{out} \sim \mathcal{N}(\mu_{out}, \sigma_{out}^2)$.

Finally, in line with [41], the average BER is computed as:

$$P_e = \frac{1}{4} \left[\operatorname{erfc} \left(\frac{\Theta - \mu_{out}}{\sqrt{2\sigma_{out}^2 |_{b=0}}} \right) + \operatorname{erfc} \left(\frac{\mu_{out} + C_{max}^{b=1} - \Theta}{\sqrt{2\sigma_{out}^2 |_{b=1}}} \right) \right], \quad (10)$$

where the transmitted bits b are independent and equally distributed, Θ is the detection threshold, and $C_{max}^{b=1} = e^{-k_r T} k_f R \int_0^T c(\tau) e^{k_r \tau} d\tau$ is the maximum number of received molecules without the noise when a 1-bit is emitted.

IV. THE OPTIMIZATION PROBLEM

Considering the relationship between the transmission power and the load current reported in (2), we formulate an optimization problem that chooses the sequence of load

$$\begin{aligned}
R_{n_{out}}(t_1, t_2) &= (\alpha^2 + \beta)H(0) \int_{-\infty}^{+\infty} h(t_1 - \nu) d\nu + H(0) \int_{-\infty}^{+\infty} \sigma_D^2(\nu) h(t_1 - \nu) d\nu = \\
&= \frac{k_f^2 R^2}{k_r} \left[(\alpha^2 + \beta) e^{-k_r t_1} \int_{-\infty}^{t_1} e^{k_r \nu} d\nu + \frac{Q}{(4\pi D)^{3/2} V_{rx}} e^{-k_r t_1} \int_0^{t_1} \frac{e^{-\frac{d^2}{4D\nu}}}{\nu^{3/2}} e^{k_r \nu} d\nu \right] = \\
&= \alpha^2 \frac{k_f^2 R^2}{k_r^2} + \beta \frac{k_f^2 R^2}{k_r^2} + \frac{Q}{(4\pi D)^{3/2} V_{rx}} \frac{k_f^2 R^2}{k_r} e^{-k_r t_1} \int_0^{t_1} \frac{e^{-\frac{d^2}{4D\nu}}}{\nu^{3/2}} e^{k_r \nu} d\nu.
\end{aligned} \tag{7}$$

currents $i(t_j)$ for $j = 1, \dots, M$ frame-by-frame, starting from a very limited subset of possible values (i.e., $i(t_j) \in \{0, i_l, i_h\}$) in order to preserve the simplicity of the transmitter. Along with a low-level and a high-level of the load current, we also consider a 0-value, which can be chosen when the amount of available energy is not enough to transmit the frame and ensure the expected BER level. The sequence of load current values is selected in order to simultaneously minimize the number of enqueued packets and the probability that the voltage in the ultra-nanocapacitor is lower than a value ϵ at the beginning of the successive ON time (i.e., $q(t_{k+1})$ and $Pr(V_c(t_{k+1}) \leq \epsilon)$, respectively), while also fulfilling energy constraints (i.e., $V_c(t_{j+1}) \geq 0$) and target BER (i.e., $P_e(j) \leq \hat{P}_e$). In each ON time period, the first frame is used by the transmitter to communicate information about the selected load currents for the successive frames. This way the receiver can calculate the transmission power in each frame for 1) eliminating the bias generated by the inter-symbol interference that produces non-zero average noise and 2) optimizing the threshold value frame-by-frame.

The optimization problem is solved by a remote nano-device with higher computational capabilities [12]: starting from system parameters, such a device obtains the optimal sequence of load currents and delivers it to the nano-transmitter. The molecular communication considered herein is static, i.e., the conditions of the channel (communication distance, diffusion coefficient, etc.) remain constant during the ON period. This prevents the related problems due to parameter changes involved in the optimization problem. Furthermore, the communication with the remote nano-device can take place before each t_{ON} period, communicating all the load current values to be used in the successive frames. This way, this information exchange is performed during the t_{OFF} periods, thus avoiding data processing and propagation delays. Without loss of generality, this work supposes to communicate the channel conditions only during the first t_{OFF} , while transmitting only the transmitter status (i.e., number of enqueued packets and amount of available energy) during the following t_{OFF} periods. Hence, the amount of energy consumed during the t_{OFF} periods is supposed to be negligible compared to the energy consumption due to the communication between transmitter and receiver nano-devices.

A. Formulation of the Objective Function

To formulate the optimization problem, we consider the impact of the selected load current values on the objective function, achieved through the scalarization method: at time

t_{k+1} , the weighted sum of the probability that the voltage in the ultra-nanocapacitor is lower than a target value ϵ and the number of enqueued packets is considered (i.e., $\gamma Pr(V_c(t_{k+1}) \leq \epsilon) + (1 - \gamma)q(t_{k+1})$). Here, γ is a weight assuming an arbitrary value from 0 to 1.

Theorem 3: Let the OFF time, t_{OFF} , be an exponential random variable with parameter λ_{OFF} . The probability to have at the beginning of the successive ON time an amount of voltage, $V_c(t_{k+1})$, lower than ϵ is equal to:

$$Pr(V_c(t_{k+1}) \leq \epsilon) = 1 - e^{-\lambda_{OFF}[-R_n C_n \ln((v_n - \epsilon)/\Phi)]}, \tag{11}$$

where $\Phi = (v_n - V_c(t_k))e^{-\frac{MT_f}{R_n C_n}} + (1 - e^{-\frac{T_f}{R_n C_n}})R_n \sum_{j=1}^M i(t_j)e^{-\frac{(M-j)T_f}{R_n C_n}}$.

Proof: Considering the equivalent circuit depicted in Fig. 1 and the well-known capacitor charging formulation with an initial voltage, the voltage at the beginning of the successive ON time, $V_c(t_{k+1})$, can be calculated starting from the voltage in $t_k + MT_f$:

$$\begin{aligned}
V_c(t_{k+1}) &= V_c(t_k + MT_f + t_{OFFk}) = \\
&= v_n + (V_c(t_k + MT_f) - v_n)e^{-\frac{t_{OFFk}}{R_n C_n}}.
\end{aligned} \tag{12}$$

If $M = 1$, the voltage across the ultra-nanocapacitor at the end of the frame can be simply computed through (1).

By generalizing, the voltage across the ultra-nanocapacitor at the end of M frames is $V_c(t_k + MT_f) = V_c(t_k)e^{-\frac{MT_f}{R_n C_n}} + (e^{-\frac{T_f}{R_n C_n}} - 1) \left[R_n \sum_{j=1}^M i(t_j)e^{-\frac{(M-j)T_f}{R_n C_n}} - v_n \sum_{m=0}^{M-1} e^{-\frac{mT_f}{R_n C_n}} \right]$. Moreover, given that $\sum_{m=0}^{M-1} e^{-\frac{mT_f}{R_n C_n}} = (1 - e^{-\frac{MT_f}{R_n C_n}})/(1 - e^{-\frac{T_f}{R_n C_n}})$, it can be written as:

$$\begin{aligned}
V_c(t_k + MT_f) &= v_n + (V_c(t_k) - v_n)e^{-\frac{MT_f}{R_n C_n}} + \\
&+ \left(e^{-\frac{T_f}{R_n C_n}} - 1 \right) R_n \sum_{j=1}^M i(t_j)e^{-\frac{(M-j)T_f}{R_n C_n}}.
\end{aligned} \tag{13}$$

Now, substituting (13) in (12), the amount of voltage across the ultra-nanocapacitor at t_{k+1} becomes:

$$\begin{aligned}
V_c(t_{k+1}) &= v_n + (V_c(t_k) - v_n)e^{-\frac{MT_f + t_{OFFk}}{R_n C_n}} \\
&- \left(e^{-\frac{t_{OFFk}}{R_n C_n}} - e^{-\frac{T_f + t_{OFFk}}{R_n C_n}} \right) R_n \sum_{j=1}^M i(t_j)e^{-\frac{(M-j)T_f}{R_n C_n}}.
\end{aligned} \tag{14}$$

Starting from (14), the probability that the voltage in the ultra-nanocapacitor at time t_{k+1} is lower than ϵ can be written as:

$$\begin{aligned} P_r(V_c(t_{k+1}) \leq \epsilon) &= P_r\left(v_n + (V_c(t_k) - v_n)e^{-\frac{MT_f + t_{OFFk}}{R_n C_n}}\right. \\ &\quad \left. - \left(e^{-\frac{t_{OFFk}}{R_n C_n}} - e^{-\frac{T_f + t_{OFFk}}{R_n C_n}}\right)\right. \\ &\quad \left. \times R_n \sum_{j=1}^M i(t_j) e^{-\frac{(M-j)T_f}{R_n C_n}} \leq \epsilon\right) \\ &= P_r\left(t_{OFFk} \leq -R_n C_n \ln\left(\frac{v_n - \epsilon}{\Phi}\right)\right), \end{aligned} \quad (15)$$

where $\Phi = (v_n - V_c(t_k))e^{-\frac{MT_f}{R_n C_n}} + (1 - e^{-\frac{T_f}{R_n C_n}})R_n \sum_{j=1}^M i(t_j)e^{-\frac{(M-j)T_f}{R_n C_n}}$.

It corresponds to the cumulative distribution function of the exponential random variable t_{OFF} with parameter λ_{OFF} . Accordingly:

$$P_r(V_c(t_{k+1}) \leq \epsilon) = 1 - e^{-\lambda_{OFF}[-R_n C_n \ln((v_n - \epsilon)/\Phi)]}, \quad (16)$$

which concludes the proof. ■

On the other hand, it is possible to estimate the impact of the load current values on the second element of the objective function, i.e., the number of enqueued packets at t_{k+1} .

Theorem 4: Considering the number of packet in the queue at t_k , $q(t_k)$, the sequence of load currents, $i(t_j)$, and the average number of incoming packet per second, λ_I , the number of packet enqueued at the beginning of the successive ON time can be estimated as:

$$q(t_{k+1}) = q(t_k) - \sum_{j=1}^M \frac{2 \arctan(Ki(t_j))}{\pi} + (MT_f + t_{OFFk})\lambda_I. \quad (17)$$

Proof: Starting from an initial number of enqueued packets in t_k of $q(t_k)$, the number of packet in the queue at t_{k+1} can be evaluated by taking into account the number of transmitted and incoming packets. The former is computed by considering the number of frames that can be potentially transmitted, M , minus the number of times the selected load current is equal to 0, η_0 . The latter, instead, corresponds to the average amount of frames generated and enqueued during M frames, η_I . Accordingly:

$$q(t_{k+1}) = q(t_k) - M + \eta_0 + \eta_I. \quad (18)$$

The number of times the selected load current is 0, η_0 , can be estimated through a saturation function, that is:

$$\eta_0 = M - \text{sat}(i(t_j)) = M - \sum_{j=1}^M \frac{2 \arctan(Ki(t_j))}{\pi}, \quad (19)$$

where $(2 \arctan(Ki(t_j)))/\pi$ is equal to 0 if $i(t_j) = 0$, otherwise it is equal to 1.

The average number of incoming packets η_I , instead, is described as the mean of a Poisson process with parameter λ_I , that is:

$$\eta_I = (MT_f + t_{OFFk})\lambda_I. \quad (20)$$

Thus, substituting (19) and (20) in (18), it is possible to conclude the proof. ■

B. Formulation of the Constraints

The optimization problem can be formulated by considering six constraints. The first constraint (i.e., $i(t_j) \in \{0, i_l, i_h\}$ for $j = 2, \dots, M$) allows choosing the sequence of load currents $i(t_j)$ among a limited set of three possible values. The second constraint (i.e., $i(t_j)|_{q(t_j)=0} = 0$ for $j = 2, \dots, M$) states that a load current equal to 0 must be chosen when there are no more packets to transmit and the queue is empty. The third constraint (i.e., $i(t_j) = i_l$ for $j = 1$) imposes that the first frame (i.e., the one carrying the load currents which will be used for the current ON time) is transmitted by consuming the lower current value. The fourth constraint (i.e., $P_e(j) \leq \hat{P}_e$ for $j = 1, \dots, M$), instead, allows to transmit information guaranteeing a target performance requirement. Finally, the fifth constraint (i.e., $V_c(t_{j+1}) \geq 0$ for $j = 1, \dots, M$) avoids to consume more energy than the available one.

Specifically, the fifth constraint can be explicitly written considering the generalized expression in (13), that is $V_c(t_{j+1}) = V_c(t_k + jT_f) = v_n + (V_c(t_k) - v_n)e^{-\frac{jT_f}{R_n C_n}} + (e^{-\frac{T_f}{R_n C_n}} - 1)R_n \sum_{l=1}^j i(l)e^{-\frac{(j-l)T_f}{R_n C_n}} \geq 0$. Accordingly, after a bit of algebra, it becomes:

$$\sum_{l=1}^j i(l)e^{-\frac{(j-l)T_f}{R_n C_n}} \leq \frac{v_n - (v_n - V_c(t_k))e^{-\frac{jT_f}{R_n C_n}}}{(1 - e^{-\frac{T_f}{R_n C_n}})R_n}. \quad (21)$$

It is worthwhile to note that the result of the probability in (11) makes sense only if the logarithm is a negative value. Thus, its argument must be lower than 1, that is $(v_n - \epsilon)/\Phi \leq 1$ where $\Phi = (v_n - V_c(t_k))e^{-\frac{MT_f}{R_n C_n}} + (1 - e^{-\frac{T_f}{R_n C_n}})R_n \sum_{j=1}^M i(t_j)e^{-\frac{(M-j)T_f}{R_n C_n}}$. Thus, the possible combination of $i(t_j)$ is further limited as follows:

$$\sum_{j=1}^M i(t_j)e^{-\frac{(M-j)T_f}{R_n C_n}} \geq \frac{v_n - \epsilon - (v_n - V_c(t_k))e^{-\frac{MT_f}{R_n C_n}}}{(1 - e^{-\frac{T_f}{R_n C_n}})R_n}, \quad (22)$$

representing the sixth constraint of the optimization problem.

C. Final Formulation of the Optimization Problem

Finally, considering an objective function based on (11) and (17) and the constraints formulated in Section IV-B, the resulting optimization problem to be solved is (23), where $\Phi = (v_n - V_c(t_k))e^{-\frac{MT_f}{R_n C_n}} + (1 - e^{-\frac{T_f}{R_n C_n}})R_n \sum_{j=1}^M i(t_j)e^{-\frac{(M-j)T_f}{R_n C_n}}$.

V. NUMERICAL RESULTS

The validation of the formulated analytical models and the effectiveness of the proposed solution are investigated in different conceivable scenarios through computer simulations, carried out by using MATLAB. The conducted study validates the noise contributions derived in Section III-B and evaluates the optimal sequence of load currents addressing the optimization problem, the resulting variation of the voltage across the ultra-nanocapacitor, the number of packets in the queue, the amount of energy consumed for transmission purposes, and

$$\begin{aligned}
& \min_{i(j), \forall j \in [1, M]} \gamma \left(1 - e^{-\lambda_{OFF} [-R_n C_n \ln(\frac{v_n - \epsilon}{\Phi})]} \right) + (1 - \gamma) \left(q(t_k) - \sum_{j=1}^M \frac{2 \arctan(Ki(t_j))}{\pi} + (MT_f + t_{OFFk}) \lambda_I \right) \\
& \text{s.t. } i(t_j) \in \{0, i_l, i_h\}, \quad i(t_j)|_{q(t_j)=0} = 0 \quad \forall j = 2, \dots, M \\
& \quad i(t_j) = i_l \quad \text{for } j = 1 \\
& P_e(j) \leq \hat{P}_e, \quad \sum_{l=1}^j i(l) e^{-\frac{(j-l)T_f}{R_n C_n}} \leq \frac{v_n - (v_n - V_c(t_k)) e^{-\frac{jT_f}{R_n C_n}}}{(1 - e^{-\frac{T_f}{R_n C_n}}) R_n} \quad \forall j = 1, \dots, M \quad (23) \\
& \sum_{j=1}^M i(t_j) e^{-\frac{(M-j)T_f}{R_n C_n}} \geq \frac{v_n - \epsilon - (v_n - V_c(t_k)) e^{-\frac{MT_f}{R_n C_n}}}{(1 - e^{-\frac{T_f}{R_n C_n}}) R_n}
\end{aligned}$$

TABLE I
LIST OF SIMULATION PARAMETERS

Nano-device Parameters
$R = 500$ [40], [41], [43], $k_f = 0.2 \mu\text{m}^3/\text{s}$ [40], [41], [43], $k_r = 10 \text{ s}^{-1}$ [40], [41], [43], $V_{rx} = 2000 \mu\text{m}^3$ [40], [41], [43]
Energy-Harvesting Parameters
$h_n = 6 \text{ pC}$ [29], [30], $C_n = 9 \text{ nF}$ [29], [30], $v_n = 0.42 \text{ V}$ [29], [30], $t_n = 1 \text{ s}$ [29], $\xi = 40\%$ [35], $V_c(0) = \epsilon = V_{min}$,
Communication Parameters
$D = 10^{-9} \text{ m}^2/\text{s}$ [43], $T_s = 1 \text{ s}$ [42], $T_b = 1 \text{ ms}$, $q(0) = 2 \text{ pkt}$, $\lambda_I = 0.05 \text{ pkt/s}$, $M = 10$.

the probability that the voltage is lower than ϵ . Most of state-of-the-art parameters are summarized in Table I. Results are reported as a function of the time, the weight of the objective function γ , the distance between transmitter and receiver d (ranging from $20 \mu\text{m}$ to $50 \mu\text{m}$ [42]), the average off time \bar{t}_{OFF} (chosen in the range from 50 s to 200 s), the number of bit per frame N (ranging from 10 bits to 30 bits), and the target BER (set equal to 5% or 10%). They are obtained by averaging 500 independent simulations in order to reduce the effect of statistical fluctuations.

The conceived optimization problem may not return a feasible solution in some specific configurations (e.g., high communication distances). Since the performance constraint is a firm requirement in the considered telemedicine scenario, we assume that the system turns off in the case this happens. Anyway, to demonstrate the unique ability of the proposed approach to ensure the target performance levels in feasible scenarios, registered BER values are compared against those obtained by conventional transmission schemes.

A. Optimal Threshold and Minimum Voltage

Fig. 3(a) depicts the optimal threshold calculated in every configuration in order to minimize the BER. The optimal threshold value decreases when the communication distance increases: according to the Fick's law of diffusion, the increment of the distance between transmitter and receiver causes a decrement in the number of received molecules, thus decreasing the optimal threshold value. For the same reason, the threshold decreases when the number of emitted molecules per bit decreases.

Fig. 3(b), instead, shows the minimum voltage across the ultra-nanocapacitor required to guarantee the target BER.

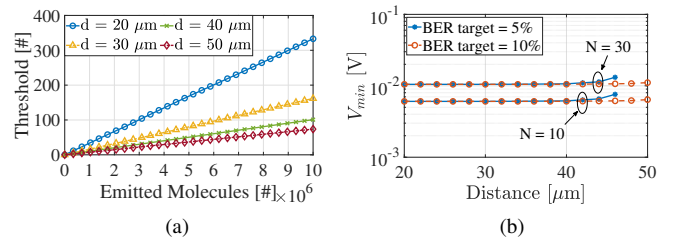


Fig. 3. (a) Optimal threshold and (b) minimum required voltage.

Since frames contain N equiprobable bits (i.e., the probability of 1-bits is equal to 0.5), V_{min} is computed by considering the minimum energy value required to transmit $N/2$ bits equal to 1 . This also fulfills the pre-defined performance level. V_{min} slightly increases up to $d = 43 \mu\text{m}$, then it increases more significantly with the communication distance, especially with lower target BER. In fact, for a given communication distance, a lower target BER requires a higher number of emitted molecules and this behavior becomes more evident when the communication is impaired by the increasing distance between transmitter and receiver. Considering that the frame is composed by $N/2$ bits, the minimum voltage per frame is higher when the frame size increases. Given the minimum voltage across the ultra-nanocapacitor, t_{ON} and t_{OFF} duration, and the size of the piezoelectric nanogenerator, a higher target BER allows higher communication distances. For target BER equal to 5% and 10% , the maximum reachable communication distance is $47 \mu\text{m}$ and $50 \mu\text{m}$, respectively.

B. Validation of the Noise Model

Simulation results in Fig. 4 validate the analytical model formulated in Section III-B. As expected from the Fick's law of diffusion, the mean and the variance for the 1-bits at the output of the receiver decrease when the communication distance increases due to the decrement in the number of received molecules. Similar results have been obtained for the 0-bit (not reported in Fig. 4 for lack of space). The mean and the variance of the noise at the output of the receiver are low with a reduced number of emitted molecules because i) the diffusion noise is strongly related to the molecule concentration reaching the receiver and ii) the inter-symbol interference depends on the number of received molecules.

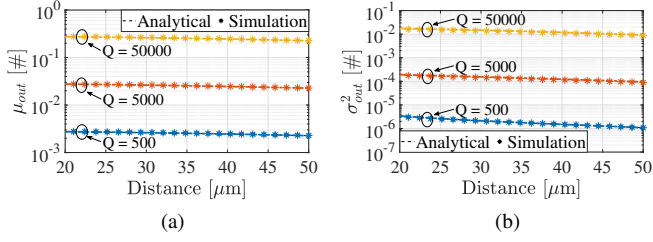


Fig. 4. Analytical/simulation results for (a) the mean, (b) the variance for 1-bits of the noise at the output of the receiver.

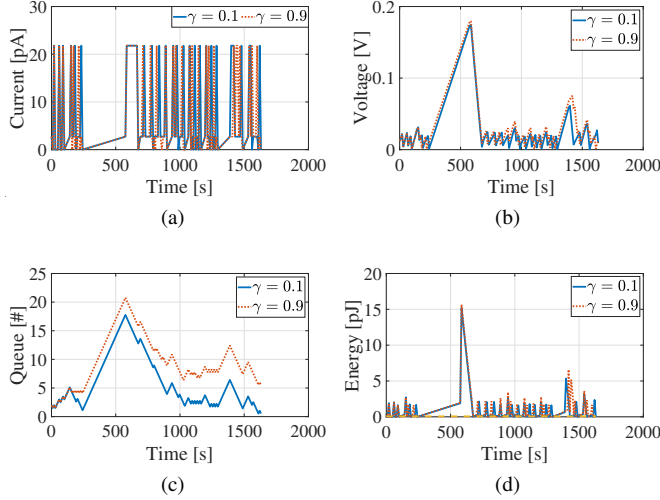


Fig. 5. Example of (a) load current sequence, (b) voltage across the ultra-nanocapacitor, (c) number of enqueued packets, and (d) consumed energy during the time, by considering two different weights γ in the objective function and setting the frame size, the communication distance, the average off time, and the target BER equal to 10 bits, 30 μm , 100 s, and 5%, respectively. The resulting voltage across the ultra-nanocapacitor and the number of enqueued packets are usually higher when a higher weight γ is used. In fact, considering the objective function in (23), a smaller weight γ mostly minimizes the number of packets in the queue, while a higher γ envisages a stricter constraint in terms of voltage. Since the voltage across the ultra-nanocapacitor increases with γ , also the energy consumed for transmission purposes is usually higher. Finally, the energy consumed for packets transmission is always higher than the minimum energy value required to accomplish performance requirements.

C. Behavior of the Optimization Problem

Fig. 5 illustrates the behavior of the obtained communication system for a single realization, reported in terms of load current, voltage across the ultra-nanocapacitor, number of enqueued packets, and consumed energy during the time, by considering two different weights γ in the objective function and setting the frame size, the communication distance, the average off time, and the target BER equal to 10 bits, 30 μm , 100 s, and 5%, respectively. The resulting voltage across the ultra-nanocapacitor and the number of enqueued packets are usually higher when a higher weight γ is used. In fact, considering the objective function in (23), a smaller weight γ mostly minimizes the number of packets in the queue, while a higher γ envisages a stricter constraint in terms of voltage. Since the voltage across the ultra-nanocapacitor increases with γ , also the energy consumed for transmission purposes is usually higher. Finally, the energy consumed for packets transmission is always higher than the minimum energy value required to accomplish performance requirements.

D. Average Performance of the Optimization Problem

The average performance levels are obtained by setting γ to 0.5, hence by giving the same priority to the probability that the voltage across the ultra-nanocapacitor is lower than a target value and the number of enqueued packets.

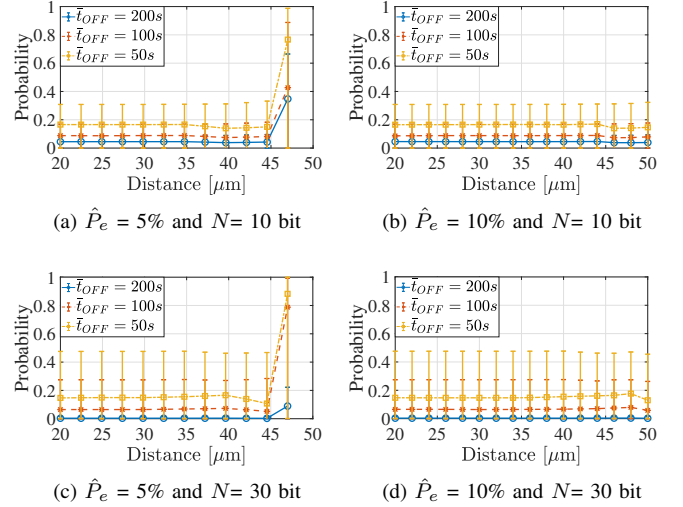


Fig. 6. Probability that the voltage across the ultra-nanocapacitor is lower than ϵ as a function of d , \bar{t}_{OFF} , \hat{P}_e , and N .

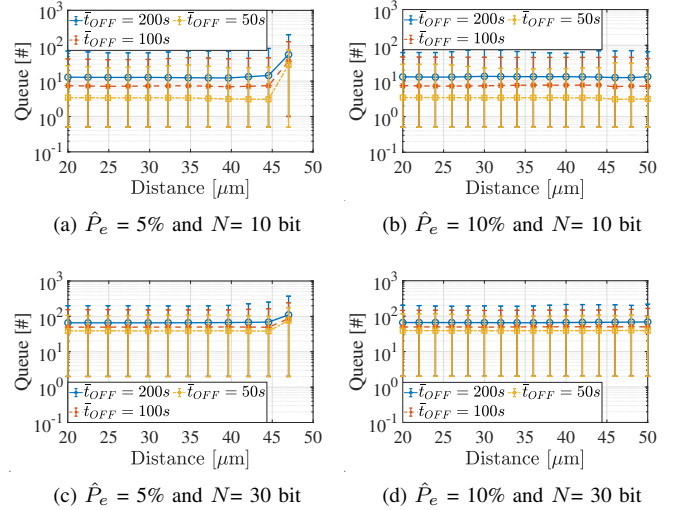


Fig. 7. Number of enqueued packets as a function of d , \bar{t}_{OFF} , \hat{P}_e , and N .

1) *Voltage probability*: Considering the voltage across the ultra-nanocapacitor, the probability that this value goes under a target voltage ϵ is illustrated in Fig. 6. This probability maintains a similar value for lower communication distance, while drastically increases when the target BER is equal to 5% and the communication distance exceeds 45 μm . In fact, a higher distance between transmitter and receiver requires an increment of transmitted molecules and, in turns, of consumed energy in order to accomplish strict constraints in terms of BER, inevitably reducing the voltage across the ultra-nanocapacitor. When the target BER is higher or the communication distance is lower than 45 μm , instead, it is possible to guarantee the performance requirements with lower number of transmitted molecules (i.e., lower consumed energy). On the other hand, the probability of a voltage lower than ϵ is always higher with lower average off time. Indeed, a higher off time allows the transmitter to retrieve more energy

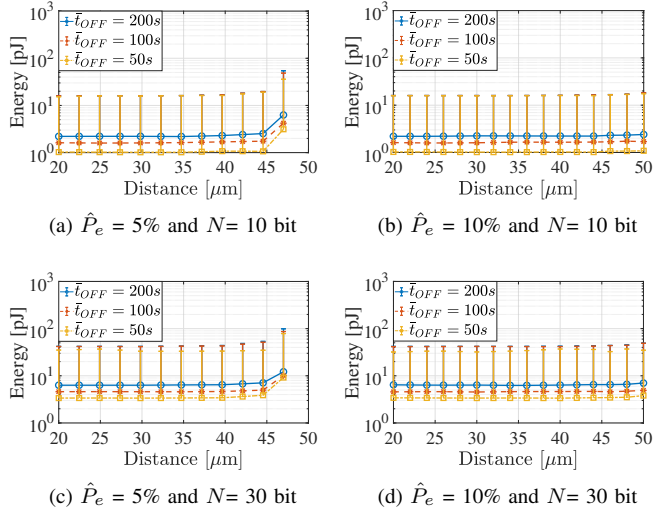


Fig. 8. Consumed energy as a function of d , \bar{t}_{OFF} , \hat{P}_e , and N .

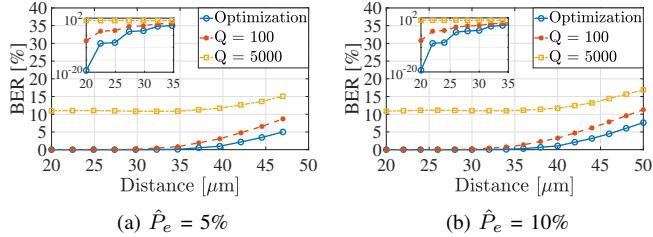


Fig. 9. BER as a function of d , \hat{P}_e , when $\bar{t}_{OFF} = 100$ s and $N = 30$ bit.

and the voltage across the ultra-nanocapacitor is higher as well.

2) *Enqueued packets*: Fig. 7 depicts the behavior of the number of packets in the queue. In particular, the increasing of the communication distance usually leads to a growing enqueued packets due to the increment of the required energy to transmit each frame. Moreover, higher number of enqueued packets are obtained for higher frame sizes. In this case, the transmitter has to manage the available energy to emit an increasing number of molecules in order to guarantee performance requirements and simultaneously minimize both the probability that the voltage across the ultra-nanocapacitor goes under the threshold ϵ and the number of enqueued packets. Accordingly, in this extreme scenario, the transmitter chooses more frequently the zero load current, thus collecting more packets in the queue. Moreover, as expected from Eq. (20), the number of incoming packets η_I grows with the increment of \bar{t}_{OFF} , thus increasing the number of total enqueued packets.

3) *Consumed Energy*: Results reported in Fig. 8 show the amount of energy consumed for the transmission process starting from the selected sequence of load currents for each configuration. The energy consumption maintains a similar value up to 45 μm , while it increases for higher communication distances and higher frame sizes. As already explained, when the distance between transmitter and receiver exceeds 45 μm , the number of information molecules required to properly transmit 1-bits and guarantee performance requirements inevitably grows, leading to an increasing energy consumption.

For the same reason, a lower target BER usually demands more effort in terms of consumed energy. At the same time, a higher number of bits per frame causes an increment of the number of molecules to be transmitted per frame and, in turns, higher energy consumption. The amount of consumed energy is also higher when a high value of off time is used. In this case, in fact, the transmitter has more time to retrieve energy, thus increasing the amount of available and consumed energy.

4) *Resulting BER*: Fig. 9 presents the resulting BER when the average \bar{t}_{OFF} is equal to 100 s and $N = 30$ bit. As expected, the measured BER increases with the communication distance because of the reduced number of molecules reaching the receiver and the high impact of both diffusion noise and inter-symbol interference. Note that a higher target BER allows to reach an increasing communication distance: the maximum tested communication distance (i.e., 50 μm) can be reached only when the target BER is set to 10%, otherwise the maximum reachable communication distance for a target BER equal to 5% is 47 μm . Moreover, the behavior of the proposed approach has been compared against conventional communication schemes encoding the symbol 1 through a burst of a constant number of molecules. Without loss of generality, the study considers static transmission scheme where $Q = 100$ [23] and $Q = 5000$ [37]. The results reported in Fig. 9 demonstrate that conventional transmission schemes are able to guarantee the target performance level only when the number of emitted molecules and the communication distance are very low (i.e., $Q = 100$ and $d < 42$ μm when the target BER is 5% and $Q = 100$ and $d < 48$ μm when the target BER is 10%). Instead, when the number of emitter molecules is high (i.e., $Q = 5000$), most of the time the transmission process fails (i.e., the receiver does not receive any molecules and decodes all the bits of the frame as 0-bits) because of the limited, or at most absent, energy budget. Definitely, the proposed investigation demonstrates the unique ability of the conceived solution to ensure the expected target BER.

VI. CONCLUSIONS

In this paper, we proposed an optimized and energy-harvesting transmission scheme for a diffusion-based molecular communication system. The developed approach dynamically selects the number of molecules to release on a per-frame basis, while satisfying energy and performance constraints. To properly define objective function and constraints, we analytically derived the mean and the variance of the aggregated noise at the output of the receiver, the probability that the voltage across the ultra-nanocapacitor goes under a target value, and the number of enqueued packets based on the behavior of the transmission process. The main lessons learned are: computer simulations validated the formulated analytical models, a higher maximum communication distance can be reached for higher target Bit Error Rate, the proposed methodology has the unique ability of fulfilling the target Bit Error Rate, while also guaranteeing the transmitter simplicity and energy requirements. Future works will explore the effectiveness of the proposed approach in more complex scenarios handling multiple communications, heterogeneous transmission techniques, variable system requirements, and different reactive

receiver models. Moreover, considering the current possibility to implement every single part of the conceived optimized and energy-harvested nano-device, it is reasonable to consider the practical implementation and test of the approach presented in this paper as another future activity.

REFERENCES

- [1] K. Yang, D. Bi, Y. Deng, R. Zhang, M. M. U. Rahman, N. A. Ali, M. A. Imran, J. M. Jornet, Q. H. Abbasi, and A. Alomainy, "A Comprehensive Survey on Hybrid Communication in Context of Molecular Communication and Terahertz Communication for Body-Centric Nanonetworks," *IEEE Trans. Mol. Biol. Multi-Scale Commun.*, vol. 6, no. 2, pp. 107–133, 2020.
- [2] M. Kuscü, E. Dinc, B. Bilgin, H. Ramezani, and O. Akan, "Transmitter and Receiver Architectures for Molecular Communications: A Survey on Physical Design With Modulation, Coding, and Detection Techniques," *Proc. IEEE*, 2019.
- [3] Q. Li and H. Li, "A Receiver Design for Molecule Shift Keying Modulation in Diffusion-Based Molecular Communications," in *Proc. of IEEE Int. Conf. on Communications in China (ICCC)*, 2019, pp. 261–265.
- [4] Q. Li, "A Novel Time-Based Modulation Scheme in Time-Asynchronous Channels for Molecular Communications," *IEEE Trans. Nanobiosci.*, vol. 19, no. 1, pp. 59–67, 2019.
- [5] Y. Huang, M. Wen, L.-L. Yang, C.-B. Chae, and F. Ji, "Spatial Modulation for Molecular Communication," *IEEE Trans. Nanobiosci.*, vol. 18, no. 3, pp. 381–395, 2019.
- [6] M. Ş. Kuran, H. B. Yilmaz, T. Tugcu, and B. Özerman, "Energy Model for Communication via Diffusion in Nanonetworks," *Nano Commun. Netw.*, vol. 1, no. 2, 2010.
- [7] N. Farsad, H. B. Yilmaz, C. Chae, and A. Goldsmith, "Energy Model for Vesicle-based Active Transport Molecular Communication," in *Proc. of IEEE ICC*, May 2016.
- [8] T. Nakano, Y. Okaie, and A. V. Vasilakos, "Transmission Rate Control for Molecular Communication among Biological Nanomachines," *IEEE J. Sel. Areas Commun.*, vol. 31, no. 12, 2013.
- [9] B. C. Akdeniz, A. E. Pusane, and T. Tugcu, "Optimal Reception Delay in Diffusion-Based Molecular Communication," *IEEE Commun. Lett.*, vol. 22, no. 1, Jan 2018.
- [10] H. K. Rudsari, M. R. Javan, M. Orooji, N. Mokari, and E. A. Jorswieck, "Multiple-Type Transmission Multiple-Type Reception Framework on Molecular Communication," *IEEE Wireless Commun. Lett.*, vol. 9, no. 11, 2020.
- [11] X. Chen, M. Wen, C.-B. Chae, L.-L. Yang, F. Ji, and K. K. Igorevich, "Resource allocation for multi-user molecular communication systems oriented to the internet of medical things," *IEEE Internet Things J.*, 2021.
- [12] S. K. Tiwari, T. R. T. Reddy, P. K. Upadhyay, and D. B. Da Costa, "Joint optimization of molecular resource allocation and relay positioning in diffusive nanonetworks," *IEEE Access*, vol. 6, 2018.
- [13] Y. Fang, A. Noel, N. Yang, A. W. Eckford, and R. A. Kennedy, "Symbol-by-symbol maximum likelihood detection for cooperative molecular communication," *IEEE Trans. Commun.*, vol. 67, no. 7, 2019.
- [14] L. Chouhan, N. Varshney, and P. K. Sharma, "On Gradient Descent Optimization in Diffusion-Advection Based 3-D Molecular Cooperative Communication," *IEEE Trans. Nanobiosci.*, vol. 19, no. 3, 2020.
- [15] N. Tavakkoli, P. Azmi, and N. Mokari, "Optimal positioning of relay node in cooperative molecular communication networks," *IEEE Trans. Commun.*, vol. 65, no. 12, 2017.
- [16] L. Chouhan, P. K. Sharma, and N. Varshney, "Optimal transmitted molecules and decision threshold for drift-induced diffusive molecular channel with mobile nanomachines," *IEEE Trans. Nanobiosci.*, vol. 18, no. 4, 2019.
- [17] V. Musa, G. Piro, L. A. Grieco, and G. Boggia, "A Lean Control Theoretic Approach to Energy-Harvesting in Diffusion-Based Molecular Communications," *IEEE Commun. Lett.*, vol. 24, no. 5, 2020.
- [18] V. Musa, G. Piro, L. A. Grieco, and G. Boggia, "A Feedback Control Strategy for Energy-Harvesting in Diffusion-Based Molecular Communication Systems," *IEEE Trans. Commun.*, vol. 69, no. 2, 2021.
- [19] M. Pierobon and I. F. Akyildiz, "Diffusion-Based Noise Analysis for Molecular Communication in Nanonetworks," *IEEE Trans. Signal Process.*, vol. 59, no. 6, 2011.
- [20] H. Shahmohammadian, G. G. Messier, and S. Magierowski, "Nano-Machine Molecular Communication over a Moving Propagation Medium," *Nano Commun. Netw.*, vol. 4, no. 3, 2013.
- [21] J.-T. Huang and C.-H. Lee, "On Capacity Bounds of Two-Way Diffusion Channel with Molecule Harvesting," in *Proc. IEEE ICC*, 2017.
- [22] H. G. Bafghi, A. Gohari, M. Mirmohseni, G. Aminian, and M. Nasiri-Kenari, "Diffusion-Based Molecular Communication with Limited Molecule Production Rate," *IEEE Trans. Mol. Biol. Multi-Scale Commun.*, 2019.
- [23] Y. Deng, W. Guo, A. Noel, A. Nallanathan, and M. ElKashlan, "Enabling Energy Efficient Molecular Communication via Molecule Energy Transfer," *IEEE Commun. Lett.*, vol. 21, no. 2, Feb 2017.
- [24] W. Guo, Y. Deng, H. B. Yilmaz, N. Farsad, M. ElKashlan, A. Eckford, A. Nallanathan, and C. Chae, "SMIET: Simultaneous Molecular Information and Energy Transfer," *IEEE Wireless Commun.*, vol. 25, no. 1, February 2018.
- [25] J. Briscoe, N. Jalali, P. Woolliams, M. Stewart, P. M. Weaver, M. Cain, and S. Dunn, "Measurement Techniques for Piezoelectric Nanogenerators," *Energy & Environmental Science*, vol. 6, no. 10, 2013.
- [26] X. Niu, W. Jia, S. Qian, J. Zhu, J. Zhang, X. Hou, J. Mu, W. Geng, J. Cho, J. He *et al.*, "High-Performance PZT-Based Stretchable Piezoelectric Nanogenerator," *ACS Sustainable Chemistry & Engineering*, vol. 7, no. 1, 2018.
- [27] S. Mohrehkesh, M. C. Weigle, and S. K. Das, "Energy Harvesting in Electromagnetic Nanonetworks," *Computer*, vol. 50, no. 2, Feb 2017.
- [28] W. Jia, G. Valdés-Ramírez, A. J. Bandothkar, J. R. Windmiller, and J. Wang, "Epidermal Biofuel Cells: Energy Harvesting from Human Perspiration," *Angewandte Chemie International Edition*, vol. 52, no. 28, 2013.
- [29] J. M. Jornet and I. F. Akyildiz, "Joint Energy Harvesting and Communication Analysis for Perpetual Wireless Nanosensor Networks in the Terahertz Band," *IEEE Trans. Nanotechnol.*, vol. 11, no. 3, 2012.
- [30] S. Canovas-Carrasco, A.-J. Garcia-Sanchez, and J. Garcia-Haro, "On the Nature of Energy-Feasible Wireless Nanosensor Networks," *Sensors*, vol. 18, no. 5, 2018.
- [31] —, "A Nanoscale Communication Network Scheme and Energy Model for a Human Hand Scenario," *Nano Commun. Netw.*, vol. 15, 2018.
- [32] S. A. Wirdatmadja, M. T. Barros, Y. Koucheryavy, J. M. Jornet, and S. Balasubramaniam, "Wireless Optogenetic Nanonetworks for Brain Stimulation: Device Model and Charging Protocols," *IEEE Trans. NanoBiosci.*, vol. 16, no. 8, Dec 2017.
- [33] M. Donohoe, B. Jennings, J. M. Jornet, and S. Balasubramaniam, "Nanodevice Arrays for Peripheral Nerve Fascicle Activation Using Ultrasound Energy-Harvesting," *IEEE Trans. Nanotechnol.*, vol. 16, no. 6, 2017.
- [34] M. Mukherjee, H. B. Yilmaz, B. Bhowmik, J. Lloret, and Y. Lv, "Synchronization for Diffusion-Based Molecular Communication Systems via Faster Molecules," in *Proc. IEEE ICC*, May 2019.
- [35] S. P. Badwal, S. S. Giddey, C. Munnings, A. I. Bhatt, and A. F. Hollenkamp, "Emerging Electrochemical Energy Conversion and Storage Technologies," *Frontiers in chemistry*, vol. 2, 2014.
- [36] R. A. Freitas, *Nanomedicine, Volume I: Basic Capabilities*, 1st ed. Landes Bioscience, 1999.
- [37] V. Jamali, A. Ahmadzadeh, W. Wicke, A. Noel, and R. Schober, "Channel Modeling for Diffusive Molecular Communication—A Tutorial Review," *Proc. IEEE*, vol. 107, no. 7, July 2019.
- [38] W. Gao, T. Mak, and L.-L. Yang, "Molecular type spread molecular shift keying for multiple-access diffusive molecular communications," *IEEE Trans. Mol. Biol. Multi-Scale Commun.*, vol. 7, no. 1, 2020.
- [39] A. Aijaz and A. Aghvami, "Error Performance of Diffusion-Based Molecular Communication Using Pulse-Based Modulation," *IEEE Trans. NanoBiosci.*, vol. 14, no. 1, Jan. 2015.
- [40] M. Pierobon and I. F. Akyildiz, "Noise Analysis in Ligand-Binding Reception for Molecular Communication in Nanonetworks," *IEEE Trans. Signal Process.*, vol. 59, no. 9, 2011.
- [41] F. Zabini, "Spatially distributed molecular communications via diffusion: Second-order analysis," *IEEE Trans. Mol. Biol. Multi-Scale Commun.*, vol. 5, no. 2, 2019.
- [42] M. Kuscü and O. B. Akan, "Maximum Likelihood Detection With Ligand Receptors for Diffusion-Based Molecular Communications in Internet of Bio-Nano Things," *IEEE Trans. NanoBiosci.*, vol. 17, no. 1, Jan. 2018.
- [43] M. M. Al-Zu'bi and A. S. Mohan, "Modeling of Ligand-Receptor Protein Interaction in Biodegradable Spherical Bounded Biological Micro-Environments," *IEEE Access*, vol. 6, 2018.